Automation in Construction 53 (2015) 95–104

Contents lists available at ScienceDirect

Automation in Construction

journal homepage: www.elsevier.com/locate/autcon

Patch detection for pavement assessment

Stefania C. Radopoulou [a,*], Ioannis Brilakis [b]

[a] Division of Civil Engineering, Department of Engineering, University of Cambridge, ISG62, Trumpington Street, Cambridge CB2 1PZ, UK
[b] Department of Engineering, University of Cambridge, BC2-07, Trumpington Street, Cambridge CB2 1PZ, UK

ARTICLE INFO

Article history:
Received 22 July 2014
Received in revised form 27 February 2015
Accepted 5 March 2015
Available online 21 March 2015

Keywords:
Patch
Detection
Pavement assessment
Pavement defect
Automatic detection
Image processing

ABSTRACT

Pavement management systems rely on comprehensive up-to-date road condition data to provide effective decision support for short, medium and long term maintenance scheduling. However, the cost per mile of the existing condition data collection methods allows only for periodical surveys. This leads to long gaps between inspections and a focus on major roads over rural ones. Therefore, pavement condition monitoring systems that provide inexpensive frequent updates on the road condition are necessary. Such systems would require robust and automatic defect detection methods using low-cost sensors. In this paper, one such method is proposed for detecting road patches from video data acquired by the car's parking camera. A patch is initially detected based on its visual characteristics, which are: 1) it consists of a closed contour and 2) its texture is the same with the surrounding intact pavement. The patch is then passed to a kernel tracker in order to trace it in subsequent video frames. This way redetection is avoided and each patch is reported only once. The method was implemented in a C# prototype and tested with video data consisting of approximately 4000 frames collected from roads in Cambridge, UK. The results show that the suggested method has 84% precision and 96% recall.

© 2015 Elsevier B.V. All rights reserved.

1. Introduction

The National Academy of Engineering has identified "Restoring and improving urban infrastructure" as one of the Grand Challenges of Engineering in the 21st century [1]. The report emphasizes the problem of maintaining infrastructure in which streets and highways are critical transportation conduits. According to the World Bank, roads often carry more than 80% of passenger-km and over 50% of freight ton-km in a country [2]. Roads assist mobility, enable growth and contribute to economic prosperity, productivity and well-being [3].

Many reports/articles that discuss the condition of the current road network and highlight the significance of efficient road maintenance have been issued. For example, in the US roads are characterized as being in poor condition and action is necessary for improvement [4]. In the UK, 61% of the country's business leaders rate local transport networks poorly in comparison to international benchmarks, while 50% of firms believe that network conditions have deteriorated over the past five years [5]. Additionally, 43% of the UK residents rank road and pavement repair to be the second highest priority for improvement [6].

Councils in the UK invest in maintaining the road condition by splitting the allocated funds spent on local roads to 75% for maintenance and 25% for construction [6]. The former share equals to 2.3 billion pounds, and constitutes a 73% increase in cash terms since 2000. Highway infrastructure assets require attention due to their great value to the public sector [7]. The concept of asset management has resulted in savings of up to 15% in some sectors. In the case of highways, it has been reported that savings of at least 5% on budget expenses have been noted. According to the International Infrastructure Maintenance Manual (IIMM), the first requirement for an impelling asset management system is to have knowledge of the existing assets, the status of their condition and the level of service they provide [8]. Pavement condition assessment data is essential when designing, planning and choosing the appropriate road maintenance programs.

The current process for assessing pavement condition comprises of the following steps: 1) collection of raw data, 2) identification of defects and 3) defect assessment. The first step is to a large extent automated; however, the other two are mostly performed manually. With regard to pavement defects, the UK Pavement Management System (UKPMS is the national standard for management systems that assesses the condition of the local road network and plans the investment and maintenance of paved areas of roads) user manual identifies the most important and basic types as cracks (longitudinal, transverse, alligator), potholes, patches, rutting and depressions [9]. The former three can be classified as *surface defects* and the rest as *elevation defects*.

Nowadays, the most effective approach for inspecting the road network is with the use of dedicated vehicles. Accredited inspectors travel in specialized vehicles for collecting raw data in different forms with the aid of several sensors, such as laser scanners, road profilers, accelerometers, image and video cameras and positioning systems [10–15]. Laser scanners, which have a resolution of thousands of points, are used to measure the longitudinal and transverse road profiles. The output is a 2D depiction of the road (either along or perpendicular to the path of way) showing the difference in the elevation along with the chainage

* Corresponding author.
E-mail addresses: scr58@cam.ac.uk (S.C. Radopoulou), ib340@cam.ac.uk (I. Brilakis).

http://dx.doi.org/10.1016/j.autcon.2015.03.010
0926-5805/© 2015 Elsevier B.V. All rights reserved.

[12,16]. Image and video cameras, positioned either at the front or at the back of the vehicle, are used to capture the condition of the road visually and provide inspectors with image data [13,15,17].

Such vehicles are very expensive to purchase as well as to operate. The Transport Research Laboratory (TRL) in Great Britain reports prices starting from £500,000, with the cost of operation and data processing ranging from £20 to £40 per kilometer [18]. Their main advantage is that they can travel at highway speeds (up to 100 km/h) without disrupting traffic, while collecting data. However, their prohibitive purchase and operational costs lead several western countries and US states to afford just a few of them. Hence, their application is limited to the principal road network, which in the UK it only constitutes 9.6% of the country's entire network [19]. This limitation also leads to large time intervals between inspections [20] leaving the rest of the network subject to more traditional, time consuming and laborious manual survey methods [11,13]. To the knowledge of the authors, no statistics are published with regard to the specific times/man hours spent for data collection. However the difference between the two available methods is easy to understand considering that manual surveys are performed on foot [9].

The next step in the process of pavement condition assessment is the analysis of the collected data. At this stage, the pavement profiles are further processed either to produce specific parameters that will assist in the calculation of the Road Condition Indicator (RCI) [11] or to calculate the pavement roughness, which is specified by an International Roughness Index (IRI) [21]. In detail, the road is split into chunks of different lengths and the corresponding collected data is processed and collated to measure the aforementioned parameters and produce a general characterization of the specific road. This aims at realizing whether this part of the road needs further detailed investigation or not [11,13]. The digital pavement video data are manually viewed and analyzed by technicians on workstations. They visually detect and assess defects based on their own experience and guided by a manual for defects, while sitting in front of two or more monitors [21,22]. The units of measure used are meters, millimeters, square meters and number of occurrences depending on the kind of defect [22].

Although the defect evaluation is performed following well-defined guidelines and criteria, it is laborious and inevitably introduces a certain amount of subjectivity. This is of paramount importance for the outcome of the results [13,23]. Unfortunately, inspectors' level of experience is expected to influence the pavement rating [24]. Private companies provide software that can assist the above process. However, such software is complementary to the equipment that the companies provide and are not provided as stand-alone packages [12,14]. Moreover, this adds to the cost of using this approach. Specific prices are not publicly available unless interest of purchase is expressed. However it is reasonable to assume that they are expensive.

With regard to the software and the algorithms themselves, little detailed information is disclosed. In general though, the data collected from the equipment mounted on the specialized vehicles (3D laser scanners, image and video cameras, etc.) are post-processed to either provide results for all defects simultaneously or individually [12,14]. Great emphasis is given to the analysis of cracks, but other defects can also be detected with such software. However, these systems fall in the category of specialized vehicles that are very expensive to purchase and operate.

In summary the issues currently identified in the pavement condition assessment process are twofold. A vast amount of data is collected and either post-processed manually leading to great time and money consumption or analyzed with expensive software, which requires the use of specialized vehicles for the data collection. Therefore, in this paper the focus is on proposing a method that is free of such limitations. In the following section, the current state of research related in automated patch detection is presented. In addition, methods useful to the research objective are also discussed. Then, the proposed solution of detecting and tracking patches is analyzed that is using data acquired from the parking camera of the car, in order to utilize a pre-existing sensor and avoid additional costs. Such cameras usually have a resolution between 0.2 and 0.4 MP; their cost ranges from £30 to £100 and can be simulated with a machine vision camera of the same characteristics that costs around £195. The paper continues with a presentation and discussion of the experiments performed to validate the proposed method and the results obtained. The final section of the paper presents the conclusions and future work.

2. Background

Much research has been performed for overcoming the limitations of current practices and automating pavement defect detection. Extensive research has been done with respect to the defect of cracks. More specifically, methods that perform crack detection [25–33], real-time crack analysis [34–37], crack classification [32,38–42], crack depth estimation [43] and even automated crack sealing [44,45] have been proposed. Detection of other surface defects such as patching, potholes and raveling in 2D images has also been investigated. For potholes, a method that detects them in images amongst cracks [46] utilizing the characteristic of texture to distinguish each defect has been presented. Another method aiming at detecting potholes [47], tracking them in videos [48] and measuring their properties [49] has also been proposed.

For patches, a couple of methods have been found in the literature. However, these methods present several limitations. At this point, the difference between presence and detection should be noted. Presence refers to the result of a process when this is only capable of providing a yes or no answer to the question of whether an object exists in the data. Detection provides the additional information of where an object is located within the given data. Hence, some methods are restricted to only recognizing the presence of a defect and classifying images between intact and healthy pavement without specifying the defect type nor which part of the image they occupy [50]. Others that use image thresholding techniques are not capable of distinguishing patches from potholes [51–53]. Finally, a statistical second order method found in the literature detects patches, but is limited to doing so in concrete pavement images [54].

From the abovementioned methods, some [33,46] use techniques from the fields of machine learning and data mining, such as Support Vector Machines (SVM) and Artificial Neural Networks (ANN). Those fields include algorithms that aim at identifying objects by learning from data. In other words, data is used to make the algorithms “learn” a specific pattern and create a “model”/rule which will then be used for the identification of the desired object. The main benefit provided is that such algorithms remove the burden of creating the detection model from the designer. On the other hand, a lot of data is required for “learning”. Therefore, if a manual model is able to detect the object robustly, there is no need of finding data for the “learning” process. Hence, the authors decided to explore the option of creating a manual model knowing that if it fails, machine learning will be investigated.

The framework of Visual Pattern Recognition (VPR) models has been proposed for creating models to automate the detection of infrastructure-related objects [55]. The idea behind this framework is to create unique detection models by utilizing their distinctive characteristics, such as metric measurements, and geometric properties. Such models have successfully been created for the detection of air pockets in concrete structures [56], concrete columns [57] and potholes [47,49]. Amongst the features used for creating VPR models is texture.

In general, there are three major approaches of describing the texture of a region and those are structural, spectral and statistical. Structural approaches are ideal for describing textures that are characterized by image primitives like parallel lines. Spectral approaches are mainly used along with Fourier transforms for detecting high energy and narrow peaks of the spectrum. Statistical approaches are most suitable for describing smoothness, coarseness, granularity etc. of the texture [58,59].

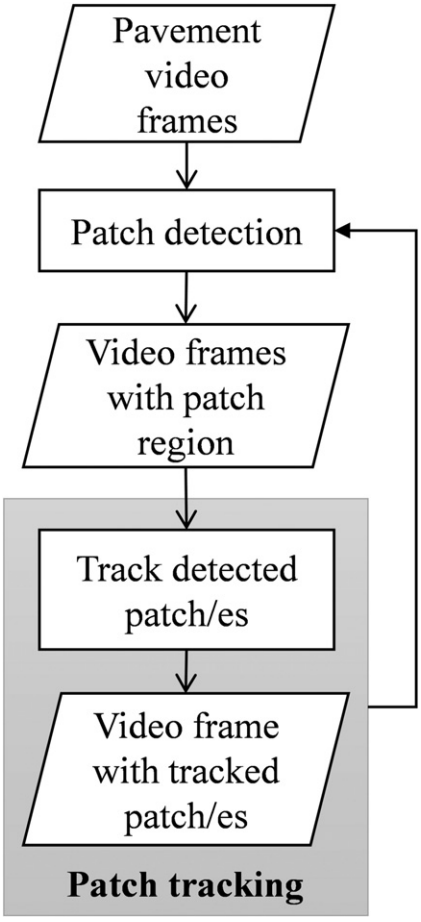

Fig. 1. Overall proposed method.

Finally, in regard to vision trackers, approaches can be categorized as contour-based, point-based and kernel-based [60]. Contour-based trackers consider the exact shape of the object and utilize edge features that are stable to illumination changes. However, such trackers show limitations with images whose edges are not strong enough to extract relevant features and have been found to be weak to illumination variations [61]. Point-based trackers utilize unique feature points of objects, but they aren't suitable for objects whose texture is very repetitive since such patterns don't have unique points to identify and match. Kernel-based methods use both the shape and appearance of the object making them quite robust. Color and texture are characteristics of the appearance of the model and kernel-based trackers use such information to track objects in video frames. Furthermore, they have the advantage of being less sensitive to illumination changes [60,62]. Finally, they have been proved to be the most suitable for detecting objects in outdoor infrastructure environments [62].

Ross et al. have proposed a 2D tracker framework that uses multi-view appearance models [63]. An object model that is capable of providing useful information about the object regions is composed of eigenimages, which are low-dimensional subspace representations acquired from previous frames. The model is updated online according to changes in appearance, such as object deformation, illumination or camera motion. At the end, a particle filter is utilized to estimate the object's motion in regard to translation, rotation, scaling and direction. The advantage of this approach is that it has been tested and validated in outdoor environments where objects undergo appearance changes due to varying illumination conditions.

In conclusion, the identified problems with the current available methods for detecting the pavement defect of patches are either associated with high costs (use of dedicated vehicles for data collection followed by their analysis from specialized software) or are limited to the level of recognition. Hence, the research question becomes: Is there an efficient and low cost approach for detecting patches? Our objective is to propose a method that is capable of detecting and tracking patches in pavement surface videos while maintaining the lowest cost possible. Such an approach will alleviate the inspector's work during the pavement assessment process, since the unit of measure used for this type of defect is the number of occurrences and the area that they cover. The scope of this paper is restricted to the detection of the defect.

3. Proposed solution

In order to address this paper's objective we are proposing a method that automatically detects patches in video frames and with the use of a vision tracker, it is able to trace them in subsequent ones. Fig. 1 depicts a flowchart of our method. The input is pavement surface video data. The reason for using such an input lies in the idea of utilizing the parking

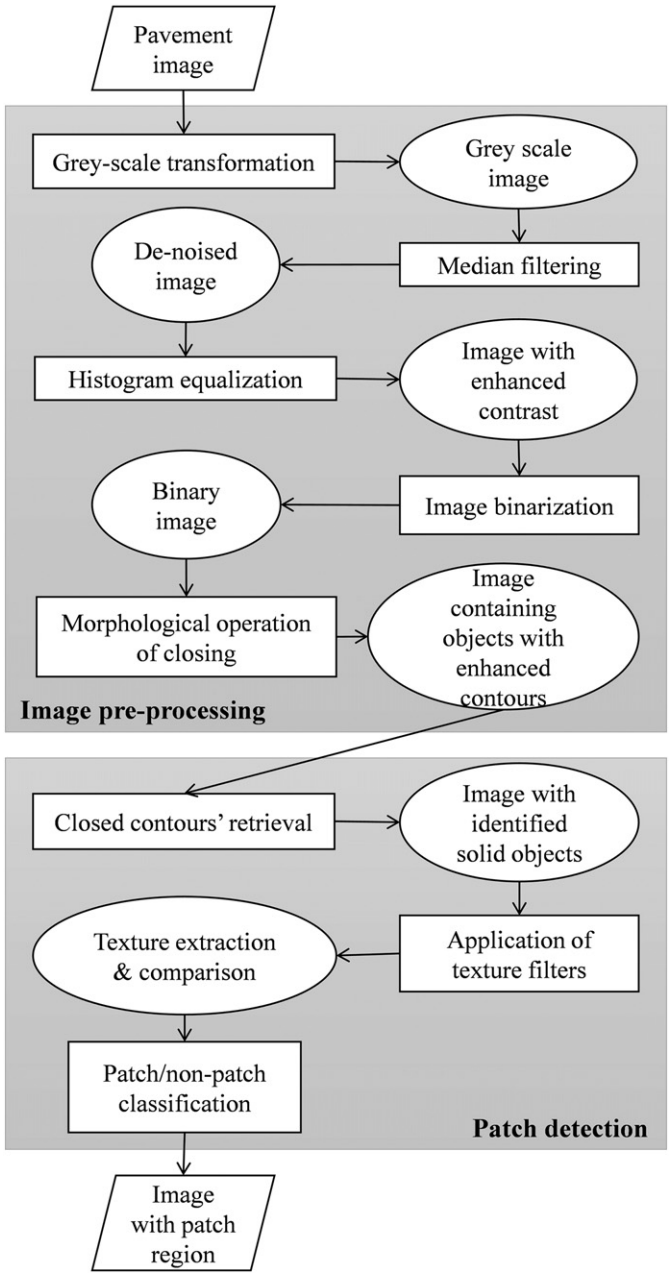

Fig. 2. Proposed patch detection method.

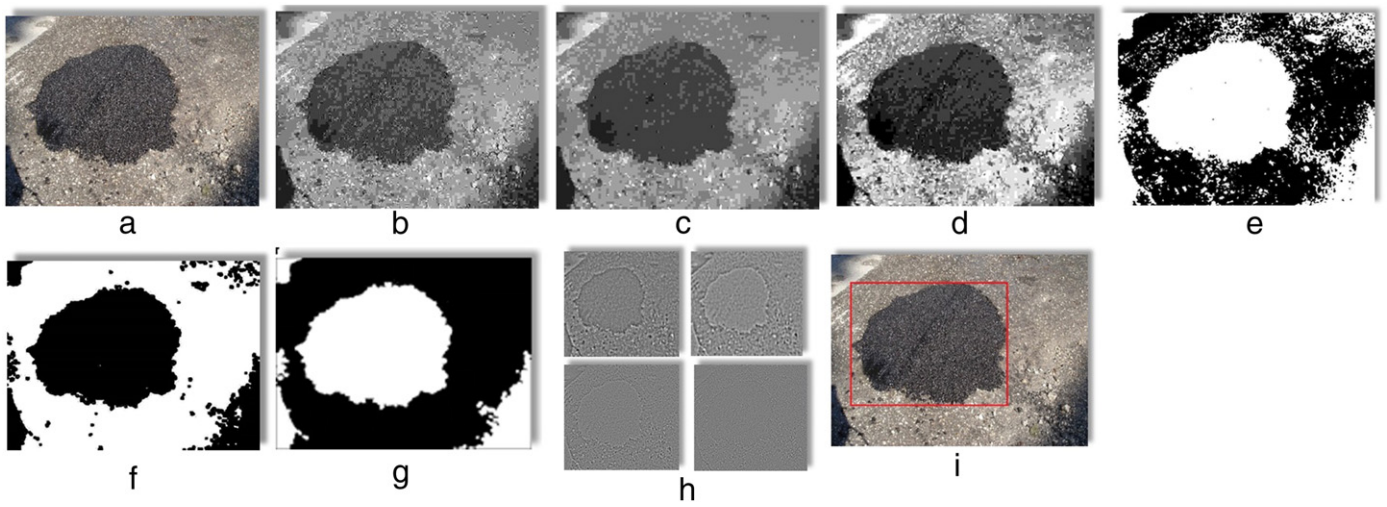

Fig. 3. The series of snapshots above illustrates the result of each stage of the proposed method. More specifically: a) initial image, b) gray image, c) de-noised image, d) enhanced image contrast, e) binary image, f) enhanced contours, g) contour regions, h) extracted texture, and i) patch in bounding box.

cameras that many cars already have installed or will be required to have in the future [64–66]. Our motivation, as mentioned above, is to propose a solution that is not expensive. If everyday road users can be transformed into ubiquitous sensors for collecting and processing data, the use of expensive dedicated vehicles or strenuous manual surveys could be eliminated. Hence, we aim at using sensors that come embedded in vehicles, which frequently travel the road, to double-up for the maintenance of the network. Furthermore, the field of view provided by such cameras is quite wide, covering not only the lane traveled, but more than that. In general, the parking cameras' angle of view is usually around 120° and sometimes goes up to 170°. Therefore, it is sufficient enough to acquire a good view of the condition of the road.

In each new video frame, patches are detected when they enter the viewport by the patch detection method (see Fig. 2). After a patch is detected, it is passed to a kernel tracker that tracks it in subsequent video frames [63]. The reason of using a tracker is to avoid detecting the same patch multiple times. The tracker is on until the patch leaves the viewport. In order for the proposed method to operate and have value, the viewport needs to depict both intact pavement and a patch or other defects as well. If only a patch is depicted in a frame, then it can't be identified because there is nothing else to differentiate it from. This is true even with naked eyes; when looking at a patch one can't tell if it is a patch or a new laid pavement. In addition, if a patch is wide enough to reach the lane markings, then it isn't categorized as a patch anymore but it is a pavement repair, which is out of the scope of this method. Finally, the above is confirmed from the ground truth data collected in which no case such as a patch covering the whole field of view was found.

The VPR models aforementioned are the inspiration for the patch detection method. Using the same strategy the patch detection method presented below is created, utilizing the following main visual characteristics of a patch:

1. It consists of a closed contour;
2. The texture of the surface of a patch is similar, if not the same, with the healthy pavement that surrounds it.

The patch detection method is split into two sub-processes: 1) image pre-processing, a step that aims at reducing the information in the image and deleting everything that is unnecessary for the purpose of the method, and 2) patch detection, the core of the detection method that is recognizing a patch and identifies the region of the image that it occupies (see Fig. 2).

In pavement surface images, color information isn't necessary. The reason is that in such an image the dominant color is gray. Hence, in order to reduce the image complexity, initially a transformation into gray-scale is applied (see Fig. 3-b). Gray-scale values range between 0, which represents black, and 255, which represents white. The process continues with the application of a 5×5 median filter used to reduce the noise in an image (see Fig. 3-c). Noise is always introduced in images by the camera during the capturing phase and because it is redundant needs to be eliminated. Therefore, the source of noise is the camera. Median filtering is chosen because it helps in reducing noise while preserving edges, which is necessary in the case of patches. As for the filter's size, it is determined based on the effect it has on the image. The larger the filter the more blurriness it produces, which is not desired (see Fig. 4). For enhancing the image, histogram equalization is then performed (see Fig. 3-d). During this process, the image intensities are redistributed along the histogram by spreading out the intensity values that are encountered the most. With this step, the contrast of the image is adjusted, which is necessary for intensifying the gray-level detail.

The process continues with making the image binary (see Fig. 3-e). This allows the separation of the darker regions of the pavement image, which in most cases represent the defective areas from the background. A patch is usually darker than the surrounding intact pavement. When a patch is initially made it is always much darker and as time passes its intensity degrades; however it still remains slightly darker. For that purpose, a histogram shape-based thresholding algorithm [67] is used. This algorithm was chosen over a pre-set/default threshold, so that the image is turned into binary using its own optimum threshold. This is usually between 90 and 120, but it depends on the intensities of the image.

The threshold value for calculating the binary image is determined as the intensity value of the histogram that has the maximum perpendicular distance to the line formed by the origin of the histogram and the point representing the maximum intensity of the histogram. All intensities that are lower (darker regions) than the threshold and represent possible defective pavement areas are set equal to 1, whereas the rest are set equal to 0. The final step in the image pre-processing step is the application of the morphological process of closing (see Fig. 3-f and Eq. (1)). With this process, contour sections tend to smooth, contour gaps tend to be filled and small holes tend to be eliminated [59]. The aim is to enhance the contours of the objects included in the image.

$$A \cdot B = (A \oplus B) \ominus B \tag{1}$$

A binary image
B structuring element. In our method a rectangle of 3×3 was used.

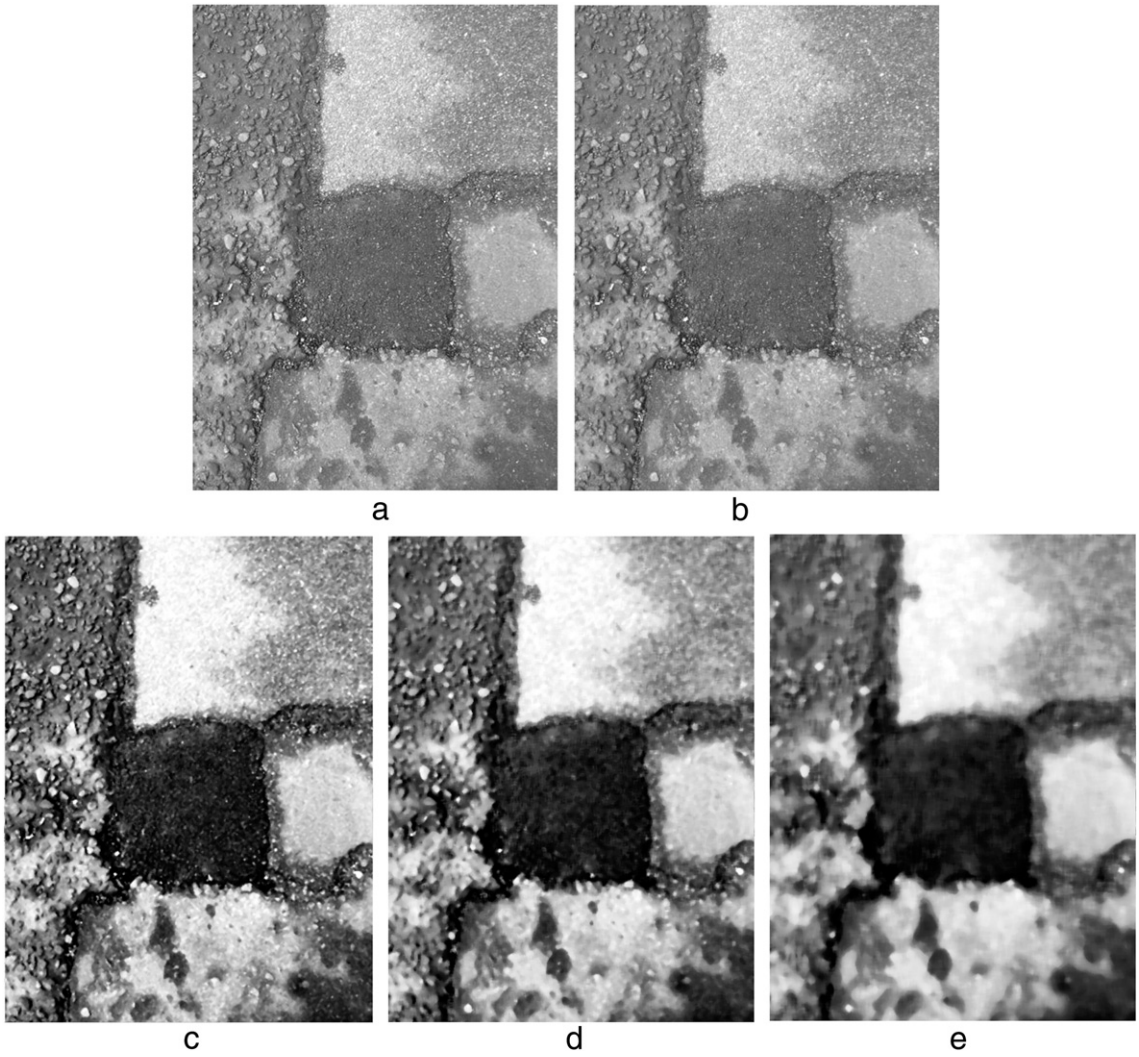

Fig. 4. Effect of different sizes of median filter to an image. (a) Original image, (b) gray image, (c) gray image after applying a 3 × 3 median filter, (d) gray image after applying a 5 × 5 median filter, (e) gray image after applying a 9 × 9 median filter.

Other sizes and shapes were also tested, but this one produced the best results without provoking any distortion.

Since it is observed that a patch is formed by a closed contour, the patch detection sub-process starts with identifying all areas formed by closed contours included in the image (see Fig. 3-g). Therefore, at this stage, whole areas formed by closed contours are detected and not only their contours. At this point, edge detectors like the Canny or Sobel operators could be used to detect the edges of objects. However, those algorithms are good for detecting edge points and since we are interested into identifying complete contours we don't use such a technique. Curvelet transformation is a popular choice for detecting curves [68], however, as stated beforehand, the goal at this stage is to detect complete contours, therefore curvelets are not chosen.

The method continues by utilizing the second visual characteristic of a patch, which is the similarity of its texture with surrounding healthy pavement. Therefore the texture of potential patch areas is compared with the texture of the surrounding intact pavement. The potential patch area(s) is/are defined by the detection of areas formed by closed contours at the previous stage of the proposed method. The rest of the image defines the surrounding intact pavement. This comparison facilitates distinguishing a patch from other closed contour elements such as manholes or objects that have fallen on the road (ex. leaves). Fig. 5 depicts the texture surface of healthy pavement and patches.

In our method, we use the standard deviation of gray-level intensity values to describe texture both for a candidate patch and the healthy pavement around it. Texture filters are applied in the original gray-level image emphasizing its structural texture characteristics (see Fig. 3-h). The responses of the filters are then used for the statistical measurement of the standard deviations. Four different filters are applied to create high filter responses. Three were taken from the filter bank of Leung and Malik [69] and one from the filter bank of Schmid [70] (see Fig. 6). The selection of those filters is based on the following reasons: First, the Leung and Malik filters were applied for material classification using texture information and the Schmid filters were used to create texture-based descriptors for content-based image retrieval. Moreover, those filters were successfully tested in images with varying lighting and viewing conditions, circumstances that also apply to pavement surface visual data. Other possible approaches would be Gabor, Gaussian or wavelet filters and Fourier analysis. However, those are mainly used for detecting edges, which isn't appropriate for this step of our process. Finally, the chosen filters have been successfully applied in the case of pothole detection [47].

Each filter is applied separately in the gray-intensity image and the standard deviations of both possible patch areas and healthy pavement

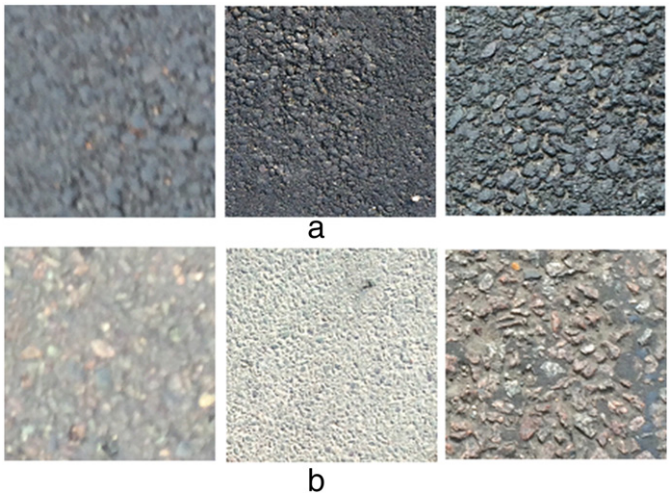

Fig. 5. Examples of the surface texture from (a) inside a patch and (b) intact pavement.

are calculated. Candidate patch areas are identified from the previous step of closed contour retrieval. Hence, two vectors of five elements each are formed. One vector includes the standard deviation values derived from the healthy pavement area and the other one the respective values derived from the candidate patch. The first element of each vector results from the standard deviation of the gray-intensity image and the other four from the standard deviation values calculated after the application of each texture filter respectively. For detecting patches, those filters and the standard deviation metric used for comparing their outcomes perform well (see following section). Therefore no other filters or approaches for describing texture were tested. Finally, a patch area is detected based on the comparison of the average values of the two vectors and the coverage of the patch (see Fig. 3-i).

The tracking part of the proposed method works as follows. When a patch is detected, its bounding box is passed to the kernel tracker. The area that is tracked is the output of the proposed patch detection algorithm. The tracker then traces the patch in subsequent frames. When the bounding box reaches the image boundary (meaning the patch is leaving the viewport) the tracking process of this patch is stopped. The patch detection algorithm runs continually in order to detect patches that enter the viewport. This method overcomes the limitation of redetecting the same patch in each frame and matching it in subsequent ones. Fig. 3 illustrates all the processing steps using as an example an image that depicts one patch.

The hypothesis tested in this paper is that the proposed method above 1) is a cheaper alternative to currently available methods for detecting patches, 2) provides accurate detection results and also 3) tackles the problem of reporting the same patch multiple times in a video sequence. The delimitations governing the proposed method are: 1) data collection is performed during the day and under natural light in sunny or cloudy condition, but not rainy and 2) the images are taken from a height that simulates the one of parking cameras positioned on the rear of vehicles.

4. Implementation and results

The performance of the method presented in this paper was tested with a C# implementation in the Microsoft Visual Studio.NET framework. It was written in Visual Studio 2010 using Windows Presentation Foundation (WPF). In addition, the publicly available Emgu CV toolbox, which is a wrapper of the Open CV library, was utilized. Both the image and the video processing were performed on a desktop PC with the following characteristics: Intel Core i7 CPU, 3.4 GHz, 8 GB RAM.

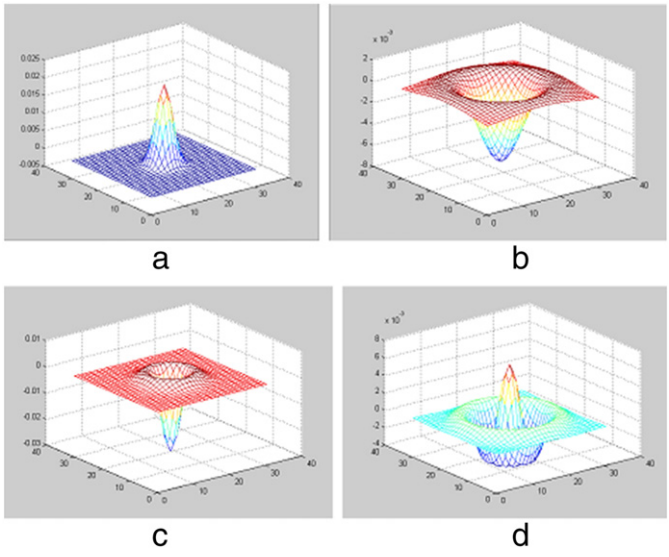

Fig. 6. (a–c) Leung–Malik spot filters and (d) Schmid spot filter.

For the validation of the patch detection method a database of 140 images was created. Half of the images were used to investigate how patches appear in images and derive rules to facilitate in their detection. The other half was used for validation. The sample size of those sets of images is determined by using Eq. (2) [71] while assuming that the database represents a common population of pavement images collected during a real pavement assessment procedure:

$$N = \frac{4z_{crit}^2 p(1-p)}{D^2}. \quad (2)$$

In this equation, z_{crit} is the standard normal deviation and is equal to 1.645. This number is derived using a significance level of 90%. The p parameter represents an estimate of the accuracy of the test and is equal to 0.5. This number is considered a worst-case scenario for sample size determination. Finally, D is the total width of expected confidence intervals and is equal to 0.2 since the significance level is set to 90%.

The database was built with images collected from the local roads of the city of Cambridge, UK. Data collection was performed under fair weather (during day light, with sunny or cloudy weather) conditions like it happens in practice. The camera's position and orientation were selected after investigating the characteristics of rear-view cameras on vehicles. With regard to their position, they are placed either just above the sign/number plate and next to the spot that lights it, or in a hole created in the upper part of the rear bumper. In the second case, in order to ensure good visibility, it is placed in the middle of the rear bumper. Different vehicle dimensions were searched and studied from the websites of manufacturers including Nissan, Volkswagen, Volvo, and Alfa Romeo. It was found that parking cameras are positioned at a height between 0.6 m and 0.9 m above the ground. The orientation is either fixed at an angle of approximately 45° or it is flexible and can be controlled by the driver.

An iPhone 5s' 8 MP camera was used. The frame size provided by this camera is 3264 × 2448 pixels. The camera was positioned at an approximate height of 0.7 m above the pavement surface and with an approximate orientation of 45°. For the validation videos a Canon VIXIA HF S100 was used. The camera was mounted on the rear of a vehicle, which was moving at a speed of 10 mph. The video data were collected at 1920 × 1090 pixel resolution, but were resized to 640 × 480 for the sake of faster processing. Aftermarket parking cameras are usually analog video sensors with low resolution that varies between 510 × 492 and 720 × 576. Hence, the size reduction of the collected videos data meets the standards of currently used parking cameras.

To measure the performance of the proposed method three metrics were used: precision, recall and accuracy. Precision is related to the detection exactness and is described by Eq. (3); recall refers to the detection completeness and is defined by Eq. (4); and accuracy refers to the average correctness of the process and is described by Eq. (5). In the equations TP stands for True Positive (correctly detected), FP stands for False Positive (incorrectly detected), TN stands for True Negative (correctly not detected) and FN stands for False Negative (incorrectly not detected).

$$\text{Precision} = \frac{TP}{TP + FP} \quad (3)$$

$$\text{Recall} = \frac{TP}{TP + FN} \quad (4)$$

$$\text{Accuracy} = \frac{TP + TN}{TP + FP + TN + FN} \quad (5)$$

As aforementioned, half of the images were used to derive rules for the characterization of a patch and how it appears within an image. The images were used to formulate the rules of coverage and texture comparison. The first refers to the boundaries set in regard to how much of the image a patch covers and it has to be between 2.5% and 65% of the image area. The second refers to the texture of the patch and the surrounding healthy pavement, for which the average values of the vectors need to be equal or have a difference no larger than 10% in order for the candidate area to be identified as a patch.

Table 1
Performance results of the patch detection method.

Performance metrics	Without texture	With texture
Total TP	37	54
Total FP	11	12
Total TN	15	9
Total FN	21	9
Accuracy	62%	75%
Precision	77%	82%
Recall	64%	86%

The detection method was first tested using 70 images of which 58 included the defect of patch. The total number of patches included in these images is 63, because some of them included more than one patch. The rest included different pavement defects such as potholes and cracks, and other objects as well, such as manholes or grating. First, we tested the detection method considering only the visual characteristic that a patch consists of a closed contour and the rule of coverage. The preliminary results were promising providing 77% precision, 64% recall and 62% accuracy. However, utilizing the additional texture information improves all three metrics significantly, providing 82% precision, 86% recall and 75% accuracy. Table 1 provides a summary of the detection method results and Fig. 7 presents patches detected in images. In regard to processing time, the detection method requires approximately 6 s (6086–6306 ms) to process an image of 3264 × 2448 pixels. pixels. In general, the processing time depends on the resolution of the image and it can be as fast as 286 ms with images of 644 × 352 pixels.

The overall proposed method (detection and tracking) was validated using pavement video data consisting of approximately 4000 video frames, including 51 patches in total. The data included other pavement defects and objects as well. The tracking accuracy refers to the patches that were successfully detected and tracked. While validating the overall process, TP is when a patch is detected successfully and tracked in all subsequent video frames until it exits the view and FP is when an area is mistakenly detected as a patch and tracked. Moreover, TP is only when the entire patch is included in the bounding box (examples are depicted in Fig. 7), otherwise it is a FP. The ability of the tracker to follow a patch and detect it in all subsequent frames without losing it, so that it is not redetected, is tested. The reason is to avoid the multiple detection of the same patch. The results show that the method presented has 84% precision and 96% recall. Table 2 presents a summary of the results. Fig. 8 depicts examples of patches detected and tracked in subsequent video frames. Regarding memory consumption, while the method is in progress it occupies 250 MB of the RAM and it processes the video at the same time that it is being played.

5. Conclusions and future work

This paper presents an automated method for detecting and tracking patches in pavement video frames. The detection of a patch is based on its main visual characteristics, which are the following; it consists of

Table 2
Performance results of overall method.

Performance metrics	#
Total TP	49
Total FP	9
Total FN	2
Precision	84%
Recall	96%

Fig. 7. Representative examples from the validation of the patch detection method.

a closed contour and second, its texture is similar to that of the surrounding healthy pavement. Additionally, the information that patch coverage within an image is between 2.5% and 65% is utilized in its detection. With regard to the tracking, this is performed with a kernel tracker. When a patch is detected, its bounding box is passed to the tracker, which in turn traces the patch in subsequent frames. When the box reaches the boundary of the image, meaning that the patch starts leaving the viewport, the tracking is stopped. However, the detection algorithm is constantly working, looking for other patches that might enter the viewport. Therefore, if a frame includes multiple patches, then those can be detected and tracked simultaneously. Moreover, if new patches enter the viewport while others are already being tracked, the new ones are detected as well and tracked in the frames to follow.

The performance was measured by comparing the method's results with the ones produced by manually identifying the ground truth. It was found that the detection algorithm has detection accuracy of 75% with 82% precision and 86% recall. As for the overall proposed method, its precision and recall are 84% and 96% respectively. Some false positives appear in the case of shadows and that is the only effect observed on the performance of the method by lighting. As for the shape of the patch, it's not believed to have any effect in the method's accuracy since the method presented is based on more general characteristics of the defect and not its shape. The results are high, revealing that the proposed method is promising and has potential. To continue, the method can be characterized as fast, since it is capable of detecting and tracking patches while the collected video is played without causing any delays or freeze outs. In regard to computational cost, it isn't expensive based on the memory it occupies while processing.

The proposed method presented in this paper focuses on the detection and tracking of patches. In future, we envisage incorporating the additional information of calculating the actual area of the patch, which is the measurement used in practice for assessing this defect. Additionally, in the visual data collected from the road network, other defects besides patches are evident. Therefore, it will be very helpful if an automated method for detecting all different kinds of pavement defects existed. Finally, road inspectors' would be further assisted in their job with the proposed method if it was coupled with a Global Positioning System device in order to provide the geospatial location of the detected defects. In this way, the problem would be pointed out

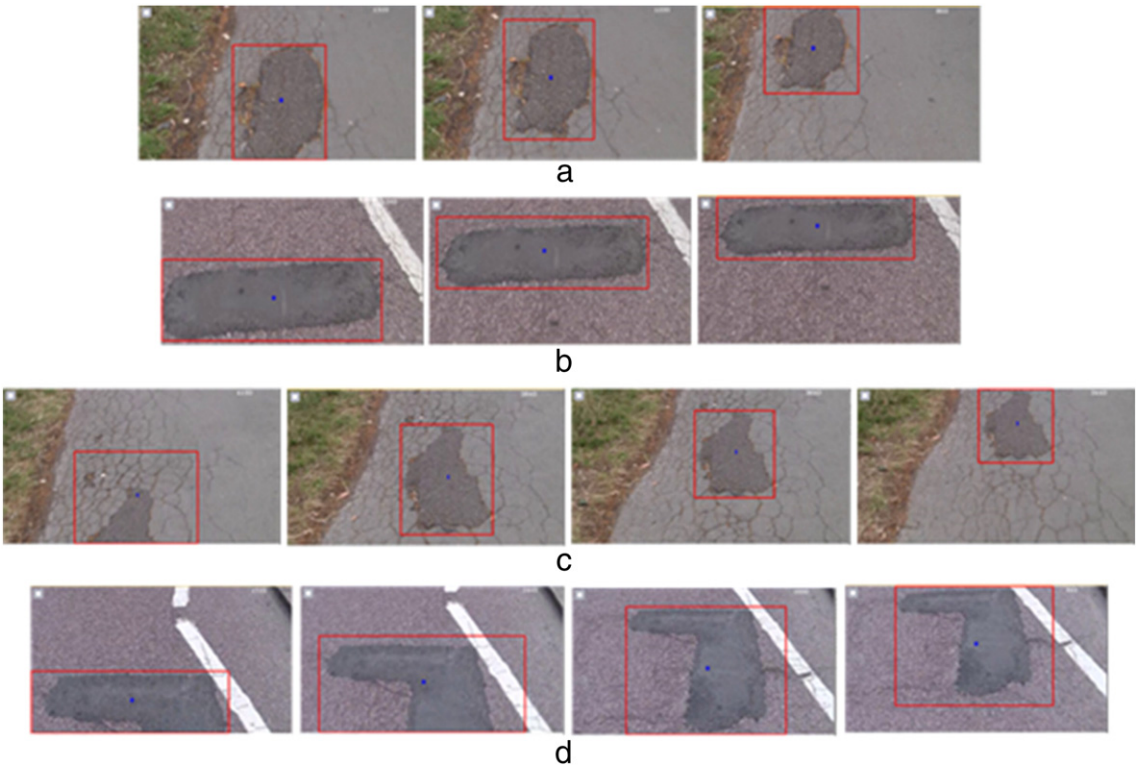

Fig. 8. Representative examples of detected and tracked patches from the validation of the proposed method.

along with its geo-tag and inspectors would be directed to specific locations of interest for more detailed analysis. Our future work will be towards those directions.

Acknowledgments

This material is based upon the work supported by the National Science Foundation (NSF Grant #1031329). Any opinions, findings, and conclusions or recommendations expressed in this material are those of the authors and do not necessarily reflect the views of the National Science Foundation.

References

[1] NAE, The Grand Challenges, 2008.
[2] The World Bank, Roads & highways, http://go.worldbank.org/MWXJNY6CC02012 (accessed June 12, 2013).
[3] A. Cook, A fresh start for the Strategic Road Network: managing our roads better to drive economic growth, boost innovation and give road users more for their money, https://www.gov.uk/government/uploads/system/uploads/attachment_data/file/4378/strategic-road-network.pdf2011 (accessed July 15, 2013).
[4] ASCE, 2013 report card for America's infrastructure, http://www.infrastructurereportcard.org2013 (accessed July 20, 2013).
[5] CBI, KPMG, Making the right connections: CBI/KPMG infrastructure survey 2011, http://www.cbi.org.uk/media/1052324/2011.09-cbi-kpmg-infrastructure-report.pdf2011 accessed July 10, 2013.
[6] audit commission, Going the distance — achieving better value for money in road maintenance, London, UK, http://www.audit-commission.gov.uk/2011/05/going-the-distance-achieving-better-value-for-money-in-road-maintenance/2011 (accessed May 26, 2014).
[7] The UK Roads Liaison Group, HMEP UKRLG highway infrastructure asset management guidance, http://www.ukroadsliaisongroup.org/en/utilities/document-summary.cfm?docid=5C49F48E-1CE0-477F-933ACBFA169AF8CB2013 (accessed May 25, 2014).
[8] NAMS Group, International Infrastructure Management Manual, National Asset Management Steering Group, 2006.
[9] UKPMS, The UKPMS user manual, http://www.pcis.org.uk/index.php?p=6/8/0/list,0,612005 (accessed June 15, 2013).
[10] Pavement Rutting Measurement With a Multi-laser Profilometer, 2011.
[11] D. for T.U. DfT, SCANNER user guide and specification, http://www.pcis.org.uk/index.php?p=6/8/0/list,0,582011 (accessed July 3, 2013).
[12] Fugro Roadware, Pavement Condition Assessment, Data Sheets, 2010. (http://www.fugroroadware.com/related/english-alldatasheets (accessed June 1, 2013).).
[13] Highways Agency, Design Manual for Roads and Bridges: Volume 7 Section 3 Part 2, Department for Transport, UK, 2008. (http://www.dft.gov.uk/ha/standards/ghost/dmrb/vol7/section3.htm.).
[14] Pavemetrics Systems Inc, Laser crack measurement system, http://www.pavemetrics.com/pdf/LCMS_flyer.pdf2013 (accessed June 18, 2013).
[15] Pavemetrics Systems Inc, Laser road imaging system, http://www.pavemetrics.com/pdf/laser_road.pdf2013 (accessed June 18, 2013).
[16] Radar Portal Systems, High Speed Laser Profiling, http://www.radarportal.com.au/surface-imaging-technology-high-speed-laser-profiling2013 (accessed June 9, 2013).
[17] R. Shekharan, Pavement Management at VDOT, 2011.
[18] P. Werro, SCANNER Surveys, 2013.
[19] D. for T.U. DfT, Technical note: road condition and maintenance data, https://www.gov.uk/government/organisations/department-for-transport/series/road-conditions-statistics2013 (accessed April 5, 2013).
[20] MnDOT, Pavement Condition Executive Summary, Minnesota Department of Transportation, 2009. (www.dot.state.mn.us/materials/pvmtmgmtdocs/execsumm_2009.pdf (accessed June 18, 2013)).
[21] MnDOT, Mn/DOT distress identification manual, http://www.dot.state.mn.us/materials/manuals/pvmtmgmt/distressmanual.pdf2003 (accessed June 2, 2013).
[22] FHWA, Distress Identification Manual for the Long-term Pavement Performance Program, Federal Highway Administration, 2003. (http://www.fhwa.dot.gov/publications/research/infrastructure/pavements/ltpp/reports/03031/01.cfm (accessed May 20, 2013)).
[23] K.A. Zimmerman, M. Stivers, A Guide to Maintenance Condition Assessment Systems, National Cooperative Highway Research Program, Urbana, Illinois, 2007. (http://maintenance.transportation.org/Documents/Final%20Report%2020-07%20Task%20206.pdf (accessed May 28, 2014)).
[24] A. Bianchini, P. Bandini, D.W. Smith, Interrater reliability of manual pavement distress evaluations, J. Transp. Eng. 136 (2010) 165–172.
[25] M. Gavilán, D. Balcones, O. Marcos, D.F. Llorca, M.A. Sotelo, I. Parra, et al., Adaptive road crack detection system by pavement classification, Sensors 11 (2011) 9628–9657.
[26] S. Ghanta, R. Birken, J. Dy, Automatic road surface defect detection from grayscale images, SPIE Smart Struct. Mater. Nondestruct. Eval. Health Monit, 2012, p. 83471E (http://proceedings.spiedigitallibrary.org/proceeding.aspx?articleid=1314842 (accessed August 17, 2013)).
[27] L. Jing, Z. Aiqin, Pavement crack distress detection based on image analysis, Mach. Vis. Hum.-Mach. Interface MVHI 2010 Int. Conf. On, 2010, pp. 576–579 (http://ieeexplore.ieee.org/xpls/abs_all.jsp?arnumber=5532588 (accessed August 17, 2013)).
[28] Q. Li, X. Liu, Novel approach to pavement image segmentation based on neighboring difference histogram method, Image Signal Process. 2008 CISP08 Congr. On, 2008, pp. 792–796 (http://ieeexplore.ieee.org/xpls/abs_all.jsp?arnumber=4566413 (accessed August 17, 2013)).
[29] C. Ma, W. Wang, C. Zhao, F. Di, Z. Zhu, Pavement Cracks Detection Based on FDWT, in: Comput. Intell. Softw. Eng. 2009 CiSE 2009 Int. Conf. On, 2009, pp. 1–4 (http://ieeexplore.ieee.org/xpls/abs_all.jsp?arnumber=5362561 (accessed August 17, 2013)).
[30] S. Sorncharean, S. Phiphobmongkol, Crack detection on asphalt surface image using enhanced grid cell analysis, Electron. Des. Test Appl. 2008 DELTA 2008 4th IEEE Int. Symp. On, 2008, pp. 49–54 (http://ieeexplore.ieee.org/xpls/abs_all.jsp?arnumber=4459508 (accessed August 17, 2013)).
[31] P. Subirats, J. Dumoulin, V. Legeay, D. Barba, Automation of pavement surface crack detection using the continuous wavelet transform, Image Process. 2006 IEEE Int. Conf. On, 2006, pp. 3037–3040 (http://ieeexplore.ieee.org/xpls/abs_all.jsp?arnumber=4107210 (accessed August 17, 2013)).
[32] Y. Sun, E. Salari, E. Chou, Automated pavement distress detection using advanced image processing techniques, ElectroInformation Technol. 2009 Eit09 IEEE Int. Conf. On, 2009, pp. 373–377 (http://ieeexplore.ieee.org/xpls/abs_all.jsp?arnumber=5189645 (accessed August 17, 2013)).
[33] G. Xu, J. Ma, F. Liu, X. Niu, Automatic recognition of pavement surface crack based on BP neural network, Comput. Electr. Eng. 2008 ICCEE 2008 Int. Conf. On, 2008, pp. 19–22 (http://ieeexplore.ieee.org/xpls/abs_all.jsp?arnumber=4740938 (accessed August 17, 2013)).
[34] Y. Huang, B. Xu, Automatic inspection of pavement cracking distress, J. Electron. Imaging 15 (2006) 013017.
[35] Y. Maode, B. Shaobo, X. Kun, H. Yuyao, Pavement crack detection and analysis for high-grade highway, Electron. Meas. Instrum. 2007 ICEMI07 8th Int. Conf. On, 2007, pp. 4–548 (http://ieeexplore.ieee.org/xpls/abs_all.jsp?arnumber=4351202 (accessed August 17, 2013)).
[36] N.T. Sy, M. Avila, S. Begot, J.-C. Bardet, Detection of defects in road surface by a vision system, Electrotech. Conf. 2008 MELECON 2008 14th IEEE Mediterr, 2008, pp. 847–851 (http://ieeexplore.ieee.org/xpls/abs_all.jsp?arnumber=4618541 (accessed August 17, 2013)).
[37] K.C. Wang, W. Gong, Real-time automated survey system of pavement cracking in parallel environment, J. Infrastruct. Syst. 11 (2005) 154–164.
[38] F. Moghadas Nejad, H. Zakeri, A comparison of multi-resolution methods for detection and isolation of pavement distress, Expert Syst. Appl. 38 (2011) 2857–2872.
[39] T.S. Nguyen, M. Avila, S. Begot, Automatic detection and classification of defect on road pavement using anisotropy measure, Proceeding EUSIPCO, 2009, pp. 617–621 (http://hal.archives-ouvertes.fr/hal-00666919/ (accessed August 17, 2013)).
[40] E. Salari, G. Bao, Pavement distress detection and severity analysis, ISTSPIE Electron. Imaging, 2011, p. 78770C (http://proceedings.spiedigitallibrary.org/proceeding.aspx?articleid=731650 (accessed August 17, 2013)).
[41] E. Teomete, V.R. Amin, H. Ceylan, O. Smadi, Digital image processing for pavement distress analyses, Proc. 2005-Cont. Transp. Res. Symp., 2005, pp. 1–13 (http://www.intrans.iastate.edu/publications/_documents/midcon-presentations/2005/TeometeDistress.pdf (accessed August 17, 2013)).
[42] L. Ying, E. Salari, Beamlet transform-based technique for pavement crack detection and classification, Comput. Aided Civ. Infrastruct. Eng. 25 (2010) 572–580.
[43] S. Amarasiri, M. Gunaratne, S. Sarkar, Modeling of crack depths in digital images of concrete pavements using optical reflection properties, J. Transp. Eng. 136 (2009) 489–499.
[44] C. Haas, Evolution of an automated crack sealer: a study in construction technology development, Autom. Constr. 4 (1996) 293–305.
[45] Y.S. Kim, H.S. Yoo, J.H. Lee, S.W. Han, Chronological development history of X–Y table based pavement crack sealers and research findings for practical use in the field, Autom. Constr. 18 (2009) 513–524.
[46] J. Lin, Y. Liu, Potholes detection based on SVM in the pavement distress image, Distrib. Comput. Appl. Bus. Eng. Sci. DCABES 2010 Ninth Int. Symp. On, 2010, pp. 544–547 (http://ieeexplore.ieee.org/xpls/abs_all.jsp?arnumber=5571563 (accessed August 17, 2013)).
[47] C. Koch, I. Brilakis, Pothole detection in asphalt pavement images, Adv. Eng. Inform. 25 (2011) 507–515.
[48] C. Koch, G.M. Jog, I. Brilakis, Automated pothole distress assessment using asphalt pavement video data, J. Comput. Civ. Eng. 27 (4) (2012) 370–378.
[49] G.M. Jog, C. Koch, M. Golparvar-Fard, I. Brilakis, Pothole properties measurement through visual 2D recognition and 3D reconstruction, Comput. Civ. Eng. 2012, 2012, pp. 553–560 (http://ascelibrary.org/doi/pdf/10.1061/9780784412343.0070 (accessed August 20, 2013)).
[50] J. Zhou, P.S. Huang, F.-P. Chiang, Wavelet-based pavement distress detection and evaluation, Opt. Eng. 45 (2006) 027007.
[51] S. Battiato, S. Cafiso, A. Di Graziano, L. Rizzo, F. Stanco, Pavement surface distress by using non-linear image analysis techniques, http://iplab.dmi.unict.it/download/Elenco%20Pubblicazioni%20(PDF)/National%20Journals%20(on-line)/simai_2006_strade.pdf2006 (accessed November 6, 2013).
[52] S. Battiato, F. Stanco, S. Cafiso, A. Di Graziano, Adaptive imaging techniques for pavement surface distress analysis, Commun. SIMAI Congr, 2007 (http://cab.unime.it/journals/index.php/congress/article/viewArticle/98 (accessed August 17, 2013)).
[53] S. Cafiso, A. Di Graziano, S. Battiato, Evaluation of pavement surface distress using digital image collection and analysis, Seventh Int. Congr. Adv. Civ. Eng, 2006 (http://iplab.dmi.unict.it/download/Elenco%20Pubblicazioni%20(PDF)/International%20Conferences/IC50%20ACE%202006%20Pavement.pdf (accessed June 4, 2014)).
[54] X. Yao, M. Yao, B. Xu, Automated detection and identification of area-based distress in concrete pavements, Seventh Int. Conf. Manag. Pavement Assets, 2008 (http://pavementmanagement.org/ICMPfiles/2008084.pdf (accessed August 17, 2013)).

[55] I. Brilakis, S. German, Z. Zhu, Visual pattern recognition models for remote sensing of civil infrastructure, J. Comput. Civ. Eng. 25 (2011) 388–393, http://dx.doi.org/10.1061/(ASCE)CP.1943-5487.0000104.
[56] Z. Zhu, I. Brilakis, Detecting air pockets for architectural concrete quality assessment using visual sensing, Electron. J. Inf. Technol. Constr. 13 (2008) 86–102.
[57] Z. Zhu, I. Brilakis, Concrete column recognition in images and videos, J. Comput. Civ. Eng. 24 (2010) 478–487.
[58] I.K. Brilakis, L. Soibelman, Y. Shinagawa, Construction site image retrieval based on material cluster recognition, Adv. Eng. Inform. 20 (2006) 443–452.
[59] R.C. Gonzalez, R.E. Woods, Digital Image Processing, 2nd SL Prentice Hall, 2002.
[60] A. Yilmaz, O. Javed, M. Shah, Object tracking: a survey, ACM Comput. Surv. CSUR. 38 (2006) 13.
[61] A. Makhmalbaf, M. Park, J. Yang, I. Brilakis, P. Vela, 2D vision tracking methods' performance comparison for 3D tracking of construction resources, Constr. Res. Congr. 2010, American Society of Civil Engineers, 2010, pp. 459–469 (http://ascelibrary.org/doi/abs/10.1061/41109%28373%2946 (accessed June 4, 2014)).
[62] M.-W. Park, A. Makhmalbaf, I. Brilakis, Comparative study of vision tracking methods for tracking of construction site resources, Autom. Constr. 20 (2011) 905–915.
[63] D.A. Ross, J. Lim, R.-S. Lin, M.-H. Yang, Incremental learning for robust visual tracking, Int. J. Comput. Vis. 77 (2008) 125–141.
[64] EU, Rear-view mirrors and supplementary devices for indirect vision (until 2014), Eur.-Summ, EU Legis, 2007.
[65] N.H.T.S.A. NHTSA, Federal Motor Vehicle Safety Standard, Rearview Mirrors; Federal Motor Vehicle Safety Standard, Low-Speed Vehicles Phase-in Reporting Requirements, 2010.
[66] C. Woodyard, NHTSA to require backup cameras on all vehicles, USA Today (2014) http://www.usatoday.com/story/money/cars/2014/03/31/nhtsa-rear-view-cameras/7114531/ (accessed May 23, 2014).
[67] P.L. Rosin, Unimodal thresholding, Pattern Recognit. 34 (2001) 2083–2096.
[68] J. Ma, G. Plonka, The curvelet transform, IEEE Signal Process. Mag. (2010) 118–133.
[69] T. Leung, J. Malik, Representing and recognizing the visual appearance of materials using three-dimensional textons, Int. J. Comput. Vis. 43 (2001) 29–44.
[70] C. Schmid, Constructing models for content-based image retrieval, Comput. Vis. Pattern Recognit. 2001 CVPR 2001 Proc. 2001 IEEE Comput. Soc. Conf. On, IEEE, 2001, p. II-39 http://ieeexplore.ieee.org/xpls/abs_all.jsp?arnumber=990922 (accessed April 16, 2014).
[71] S.C. Series, Sample size estimation: how many individuals should be studied? Radiology 227 (2003) 309–313.